Available online at www.sciencedirect.com
SCIENCE DIRECT®
Journal of Membrane Science 243 (2004) 417–424
journal of MEMBRANE SCIENCE
www.elsevier.com/locate/memsci

Time evolution of electrokinetic flow-induced streaming potential and flux in dead-end and cross-flow filtration of colloids through nanopores

Myung-Suk Chun[a,*], Wan Cheol Park[b]

[a] *Complex Fluids Research Laboratory, Korea Institute of Science and Technology (KIST), PO Box 131, Cheongryang, Seoul 130-650, South Korea*
[b] *Environment and Process Technology Division, Korea Institute of Science and Technology (KIST), PO Box 131, Cheongryang, Seoul 130-650, South Korea*

Received 16 March 2004; received in revised form 9 July 2004; accepted 12 July 2004

Abstract

The comparative behavior of particle deposition in the dead-end as well as the cross-flow filtrations was investigated with the latex colloid under different particle concentrations, where the repulsive interaction exists between membranes and particles. We found that the time evolution of the electrokinetic streaming potential during the filtration of colloids can provide useful real-time information on particle deposition onto the outer surfaces of membranes. With the progress of filtration, the magnitude of streaming potential in fully retentive pores at the dead-end mode becomes evidently decreased, whereas the opposite behavior is shown at the cross-flow one. Experimental results of the filtrate flux concerning the streaming potential indicate that both the cake layer thickness and the particle concentration in the cake layer for dead-end case show higher values than those of cross-flow one. Regardless of the filtration modes, these properties are increased with the increase of particle concentration. Compared to the dead-end filtration with flat-plate membrane, the cross-flow characteristic allows the particles to stay in a suspended state above the outer surface of hollow-fibers instead of being deposited.

Keywords: Streaming potential; Latex colloid; Dead-end filtration; Cross-flow filtration; Electrokinetics

1. Introduction

Numerous studies have been devoted to understand the behavior of filtrate flux decline due to the particle deposition onto membrane surfaces. In the fully retentive membranes, whether we employ a dead-end mode or a cross-flow mode, the retained solute particles at the membrane surface build up with time as a cake layer. The retained solutes above the cake layer result in a concentration polarization (CP) layer with the spatially variable solute concentration [1–4].

Complicated physicochemical properties of the bulk suspension of charged colloids are closely related to the development of CP layer. Besides the long-range interaction between the membrane surface and the particles, the colloidal interaction energies are necessarily involved in multiparticle interactions. Many attempts have been made at examining the osmotic pressure for colloidal suspensions with multiparticle interactions [5–7]. As a relevant study underlying these interactions, Chun et al. [8] presented effects of the expanded double layer around particle surfaces on the dead-end filtration properties, based on the estimations of the cake porosity and the cake compressibility.

Surface properties of the filtration membranes have been shown to influence filtrate flux, membrane fouling, and solute rejection. Measuring the flow-induced streaming potential based on electrokinetic phenomena became the widely used technique to characterize the electric properties of both the pore surfaces and the outer surface of the membrane [9–17]. Both the cake layer and the concentration polarization layer developed on the outer surface of the membrane influence upon the streaming potential, which suggests the significance

* Corresponding author. Tel.: +82 2 958 5363; fax: +82 2 958 5205.
E-mail address: mschun@kist.re.kr (M.-S. Chun).

0376-7388/$ – see front matter © 2004 Elsevier B.V. All rights reserved.
doi:10.1016/j.memsci.2004.07.009

of the time evolution of the streaming potential to a monitoring the fouling [18].

In this study, we investigate an explicit comparison on the cake layer formation due to particle deposition between the dead-end and the cross-flow filtrations measuring the electrokinetic streaming potential with the progress of filtration time. The mechanism of filtrate flux decline is considered based on a transient flux model. Commercially available membranes of both the flat-plate and the hollow-fiber types were chosen, and colloidal suspensions of polystyrene latex were prepared with different particle concentrations. Experimental observations are carried out for solutions at pH 8.6, in which the electrostatic repulsion exists between the fully retentive membrane pore and the particles with the same (i.e., like) charged condition. In special, observing the axial-position-dependent streaming potential identifies the effect of the concentration polarization layer generated during the cross-flow filtration.

2. Basic considerations on membrane filtrations of colloids

The streaming potential arises when a pressure difference is applied across the membrane, causing the electric double layer (EDL) to shear due to the flow of electrolyte solution which displaces the electric charges of the diffuse part of the double layer. The charge characteristics of the membrane pore walls were observed by applying the apparent streaming potential, in which the surface charges of the pore wall affect both the long-range electrostatic interactions and the formation of cake layer. Moreover, the evolution behavior of the streaming potential is available to usefully explain the flux change during the filtration of colloids.

Several mechanisms such as dissociation of surface functional groups, adsorption of ions, and adsorption of charged molecules account for the surface charge of membranes contacted with aqueous solutions. In an electric field governed by the Poisson–Boltzmann (P–B) equation, the thickness of the EDL at the phase boundary can be quantified by the Debye length. The inverse Debye length κ is defined by $\sqrt{\left(e^2 N_A \sum_i c_i^0 Z_i^2\right)/\varepsilon kT}$. Note that e is the elementary Coulombic charge, N_A the Avogadro's number, ε a dielectric constant, kT the Boltzmann thermal energy, c_i^0 the concentration of ion species i in the bulk solution (in moles per unit volume), and Z_i its valence. We consider here the condition of overall electroneutrality in an equilibrium solution. For aqueous solutions of monovalent electrolytes at 25 °C, the Debye length κ^{-1} (nm) is given by (solution ionic strength (mol))$^{-1/2}$/3.278. For a low surface potential (i.e., less than kT/e = 25.69 mV) with a 1:1 electrolyte system, the P–B equation may be linearized, which is called the Debye–Hückel equation [19,20].

Once the electrolyte solution flows through the membrane pores by means of pressure P, the ions are stripped off along the shear plane, and a streaming current is formed. Charge accumulation at the downstream side generates an electric field that causes a backflow of ions until a steady state is reached. Direct information about the electrostatic charge at the EDL shear plane is obtained in terms of the electrokinetic streaming potential E [21]. For surfaces with low surface conduction compared to the solution conduction, the fundamental relationship between the measured streaming potential E and the membrane zeta potential ζ is reasonably given by the well-known Helmholtz–Smoluchowski (H–S) equation, $\Delta E/\Delta P = \varepsilon\xi/\eta\lambda_0$, where η is the solution viscosity and λ_0 the solution conductivity [22]. The linear relationship between ΔE and ΔP can be obtained from the streaming potential difference ΔE measured with variations of the transmembrane pressure drop ΔP.

When the EDL thickness exceeds the pore radius, a rigorous analysis in terms of the H–S formula is inevitably limited. The overlap of EDL inside the membrane pore results in a concentration gradient across the pore, and subsequently the solution conductivity at the pore region will deviate from its bulk value. The membrane potential caused by this concentration gradient is added to the pressure-induced streaming potential, on which the 'filtration potential' has been acknowledged recently [23]. The streaming potential defined in this study means the apparent one, however, which allows us favorably to examine its behavior or trends in the membranes without complicated calculations.

In the membrane filtrations shown in Fig. 1, the filtrate flux v incorporating with the boundary layer model is described by the Darcy's law for the overall hydraulic resistance in terms of membrane, cake, and polarization resistance in series. With employing the effective pressure drop on both the membrane and the cake layer, the general filtration equation

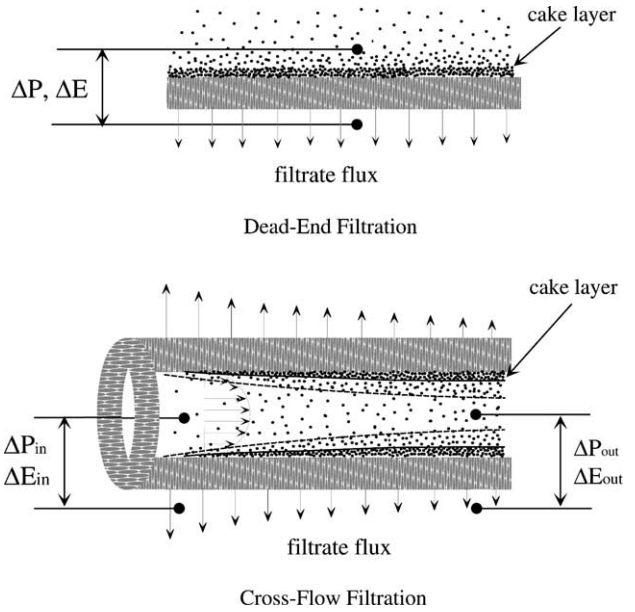

Fig. 1. Schematic representation of the dead-end filtration with flat-plate membrane and cross-flow filtration with hollow-fiber membrane.

can be expressed as [2,8]

$$v = \frac{\Delta P - \Delta P_p}{\eta(R_m + R_c)} \quad (1)$$

where ΔP is the transmembrane pressure drop imposed across the cake and the membrane, ΔP_p the pressure drop on the CP layer, R_m ($=\Delta P/\eta v_{water}$) a resistance of the clean membrane, and R_c the cake resistance. When a cake layer is present on the membrane surface, the ΔP_p is maintained at a critical value. This critical pressure is, independent of the applied pressure and the filtrate flux, solely determined by the thermodynamic properties of the suspensions. For a monodispersion, the critical pressure is determined by [24]

$$\Delta P_p = \frac{3kT}{4\pi a^3} N_{Fc} \quad (2)$$

where a is the particle radius and N_{Fc} the critical filtration number, which is 15 for uniform rigid spherical particles at a cake concentration C_c of 0.64. The particle accumulation in the cake layer provides an additional resistance to the filtrate flow, from which this resistance causes the filtrate flux to decline. When the particle diameter is larger than the pore one like the case of fully retentive, the cake resistance is likely to change alone. The cake resistance is a product of the specific cake resistance and the cake thickness, where the specific cake resistance is estimated with the Carman–Kozeny equation. Then, we have

$$R_c = \hat{R}_c \delta_c = \left(\frac{45}{a^2} \frac{C_c^2}{(1 - C_c)^3}\right) \delta_c \quad (3)$$

We adopt the assumption that the initial filtrate flux decline is independent of the longitudinal flow. This can be explained by the fact that, at the initial stages of cross-flow filtration, most particles brought to the membrane surface by filtrate flow deposit in the cake layer and the longitudinal transport of excess particles by cross-flow is negligible. Also, the particle accumulation in the CP layer is mostly assumed to reach steady state in a very short time. Then, a dead-end filtration theory provides a good approximation for the transient flux decline of cross-flow filtration.

3. Experiments

3.1. Membranes and model colloid

We used both the PM10 flat-plate membrane (Amicon, currently Millipore, MA) and the PM10 hollow-fiber membrane (Koch Membrane System Inc., MA), which are made from polysulfone. The characteristics of these asymmetric membranes are given in Table 1. The morphology of a cross-section was observed with a field emission scanning electron micrograph (FE-SEM, Hitachi Ltd., S-4200). The molecular weight cut-offs correspond to 10 kDa, and the mean diameters of the pore in the skin layer are estimated as 3.8 and 3.1 nm, respectively [18]. Each membrane was rinsed with distilled water to remove the wetting agent prior to use.

Table 1
Characteristics of membranes

Membrane	PM10 (flat-plate)	PM10 (hollow-fiber)
Hydrophilicity	Hydrophobic	Hydrophobic
Molecular weight cut-off (Da)	1×10^4	1×10^4
Mean pore diameter (nm)	3.8	3.1
Solute rejection (%)		
Polystyrene latex ($2a$ = 0.05 μm)	Above 98	Above 98
Bovine serum albumin (BSA) protein	95	95

Surface chemical characterization was carried out by X-ray photoelectron spectroscopy (XPS) using a Physical Electronics PHI 5800 spectrometer with a non-monochromatic Al Kα radiation (350 W, 15 kV, 1253.6 eV) as excitation source. High-resolution spectra were recorded at a take-off angle of 45° by a concentric hemispherical analyzer operating in constant pass energy mode (at 187.85 and 23.5 eV for wide and narrow scan, respectively), using a 400 μm diameter analysis area. Membranes were irradiated for a maximum time of 15 min to minimize sample damage. Atomic concentration percentages were determined from the different measured spectral regions by taking into account the corresponding area sensitivity factor.

As a model colloid, monodisperse polystyrene latex (Emulsion Polymer Institute, Seoul, South Korea) with a mean diameter of 0.05 μm was used. The zeta potential of latex colloid, determined using a Zeta-Plus (Brookhaven Instrument Co., NY) was calculated from the mobility values based on a Doppler principle together with the particle velocity obtained by Smoluchowski formula. Filtration experiments were carried out using latex suspensions with 1.0 mM KCl electrolyte of pH 8.6. The rejection for latex suspension was determined by a comparison of latex concentrations in the feed and in the filtrate using a UV detector (Rainin, Model Dynamax UV-1, CA). Its value results in above 98%, justifying a fully retentive behavior of PM10 membranes.

3.2. Simultaneously monitoring apparatus for filtrate flux and streaming potential

Each of the apparatus for flat-plate as well as hollow-fiber membranes was properly developed in our laboratory, with which both the *in situ* streaming potential and the filtrate flux could be measured simultaneously [25]. The effect of latex concentration has been examined with simultaneously monitoring as a time progress. Except for the streaming potential cell, both the dead-end and the cross-flow filtrations measured the filtrate flux with the same method. Pressure was supplied by a high-precision metering pump (M920, YoungLin Co., Seoul) and precisely measured by a transducer and a digital

readout. Transmembrane pressure was adjusted up to 0.3% of the maximum flow rate using a micrometer capillary valve (Gilmont Inst., IL). The amount of filtrate collected over time was determined by continuously weighing it on an electronic balance (Mettler, Model PG 502, Switzerland), and then it was registered simultaneously by data acquisition program (BalanceLink Version 2.20, Mettler-Toledo AG).

Regarding a device for streaming potential of dead-end mode, details of the system and procedure have been described elsewhere [10,11]. The streaming potential cell consists of upper and lower parts, in which a flat-plate membrane situated between them has an effective area of $\pi(1.75)^2$ cm^2. The streaming potential cell equipped with a single hollow-fiber has dimensions 0.31 cm in inner diameter and 12 cm in effective length, wherein the ends of the cell were potted with cured epoxy resin in order to place a hollow-fiber. The hollow-fiber membrane has inner diameter of 0.11 cm and outer diameter of 0.21 cm. The Ag/AgCl electrodes were prepared by anodic deposition of chloride on silver with a DC power supply (Consort E832, Belgium) at 0.4 mA/cm^2 for 40 min. The rod-type electrodes 3 mm in diameter installed in each part of the dead-end cell is desirably spaced no greater than 0.02 cm from the flat-plate membrane. Due to the origin of cross-flow through the inner channel of hollow-fiber, a measurement of the axial-position-dependent streaming potential is necessary. For this purpose, pairs of Ag/AgCl electrodes were installed very carefully both inside and outside inlet as well as outlet positions of a hollow-fiber. Actually, inlet and outlet positions are set at the locations of 1.0 cm apart from each end of the hollow-fiber. A wire-type electrode with 0.25 mm in diameter installed inside the hollow-fiber takes about 6% of the internal cross-sectional area of the hollow-fiber to allow an undisturbed flow condition. A spiral electrode is suitably installed on the corresponding external positions of the hollow-fiber so that it can detect the minute streaming potential difference.

After the system was stabilized at a given ΔP, the streaming potential difference ΔE across the membrane pore was detected using a multi-channel digital multimeter (HP34970A, Hewlett-Packard Co., CA) connected to the pairs of electrodes. In case of the cross-flow filtration, ΔE between the inside and outside of the hollow-fiber was measured for two pairs of electrodes at both inlet and outlet positions. The streaming potential difference was measured with variations of the transmembrane pressure drop, for which several discrete pressures (i.e., 4 or 5) around 2.5 bar were generated, with the system allowed to equilibrate at each pressure. Solution conductivity λ_0 was measured using a conductivity meter (Model 32, YSI, OH).

4. Results and discussion

4.1. Surface charge characterization

Relative percentages of atomic concentrations for the polysulfone characteristic elements (C, O, S) are provided in Table 2. The existence of N was obtained, and it can be seen a difference between relative percentages for the outside of the skin layer and that of the support layer. The values of C and O obtained for PM10 differ somewhat from the values either obtained for UDEL polysulfone (Union Carbide, CT) or reported in the literature [26].

Table 2
Surface atomic concentrations estimated by XPS experiments

Sample	C (%)	N (%)	O (%)	S (%)
PM10				
Flat-plate (outside of skin layer)	76.8	1.5	19.2	2.5
Flat-plate (outside of support layer)	81.6	1.8	13.9	2.7
PM10				
Hollow-fiber (outside of skin layer)	75.0	1.7	21.1	2.2
Hollow-fiber (outside of support layer)	79.9	2.4	15.3	2.4
UDEL®	84.8	1.1	11.6	2.5

We found that measurements of streaming potential were highly reproducible and a linear relationship between ΔP and ΔE can be seen for the range from 0.1 to 0.38 bar. The apparent zeta potentials of membranes related to the electrokinetic properties of the pore take the variability of less than 8%. The concentration gradient across the pore of hollow-fiber results in an initial non-linearity observed in ΔP of less than 0.1 bar. This initial non-linearity also caused by a shift in the zero-pressure intercept, due to small asymmetries in the electrodes. The conductivity of the bulk solution λ_0 shows a minimum value of $1.32 \times 10^{-2}\ \Omega^{-1}\ m^{-1}$ at pH 7.0, while it is increased with either pH decreasing or pH increasing [18]. Fig. 2 exhibits that the PM10 membranes are considered to be weakly charged compared to either the polystyrene latex or the BSA protein. The latex surfaces are always negatively charged, where its magnitude of zeta potential was greater than that of the membrane pore. The isoelectric points of pore

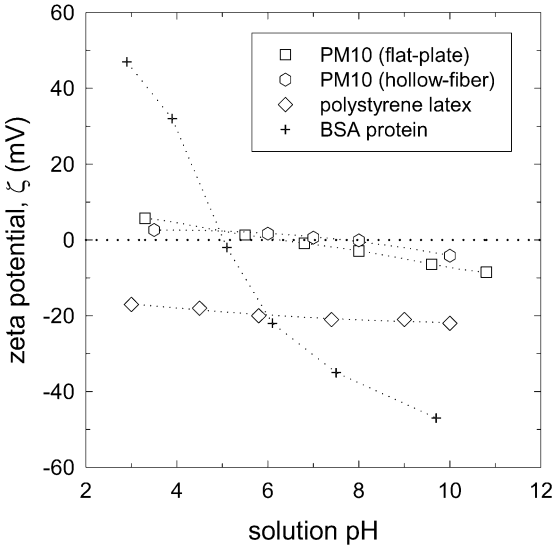

Fig. 2. The zeta potential characterization of polystyrene latex, bovine serum albumin (BSA) protein, and model membranes in 1.0 mM KCl solution; zeta potential for model membranes represents the apparent one.

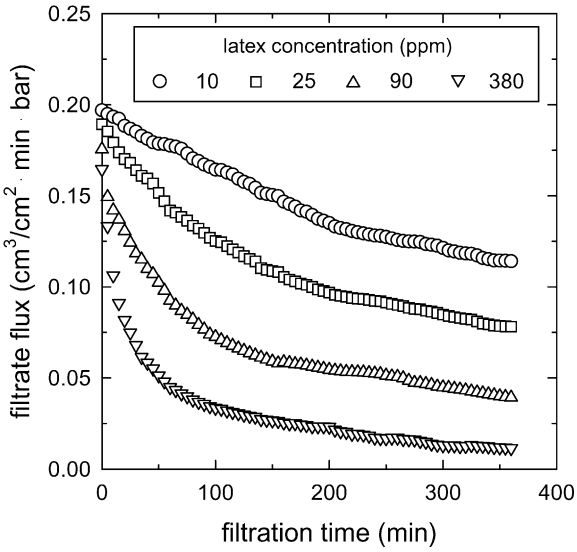

Fig. 3. Changes in the filtrate flux of flat-plate membrane during the dead-end filtration with different latex concentrations (=C_b) at pH 8.6 and 1.0 mM KCl.

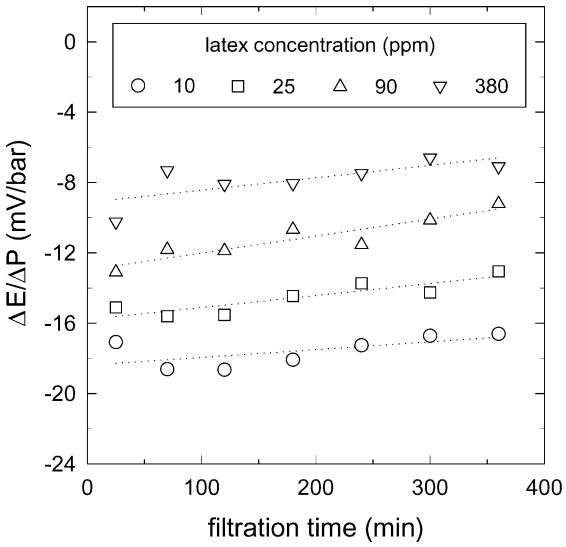

Fig. 4. Changes in the streaming potential coefficient of flat-plate membrane during the dead-end filtration with different latex concentrations (=C_b) at pH 8.6 and 1.0 mM KCl.

surfaces for flat-plate and hollow-fiber are formed around pH 6.0 and 7.4, respectively.

4.2. Comparisons between dead-end and cross-flow modes

The ionic concentration of 1.0 mM of KCl electrolyte at 25 °C corresponds to the Debye length of 9.7 nm, which is larger than the mean pore radius. We consider here the time evolution behavior instead of the rigorous estimation of the zeta potential. The surfaces of the latex particle and the pore wall employ a same-charged condition with negative charges at pH 8.6. Fig. 3 displays the variations of the filtrate flux in flat-plate membrane with the filtration time at different latex concentrations. We can recognize that the latex concentration of 10 ppm corresponds to sufficiently dilute case. As the latex concentration increases the filtrate flux decreases, in which the corresponding flux decline is also considerable.

Comparing the time evolution of the streaming potential for the same solution environments can be an efficient method of examining the filtrate flux. Fig. 4 indicates that, as the time proceeds, the absolute values of the streaming potential coefficient (=$\Delta E/\Delta P$) tend to decrease. This trend is possibly due to the direct deposition of all latex particles brought to the membrane by dead-end filtration onto the surface of the flat-plate membrane. Once the latex particles deposit, the electrokinetic flow through the fully retentive nanopore is reduced due to a development of the cake layer. With increasing the latex concentration, the absolute value of the streaming potential becomes decreased resulting from a formation of dense cake layer.

Fig. 5 shows the flux decline of the hollow-fiber membrane with cross-flow filtration mode. For dilute concentrations of 10 and 25 ppm, we observe that the filtrate flux is almost constant. Fig. 6 indicates that, in contrary to the dead-end filtration, the absolute value of the streaming potential coefficient tends to entirely increase as the time proceeds. This explains that the negatively charged latex particles hardly deposit onto the outer surface of the negatively charged hollow-fiber, since the electrostatic repulsion is effective in cross-flow filtration mode. Instead, they exist mainly as a suspended state above the hollow-fiber surface, which forms the concentration polarization layer. Large amounts of ionic charges originating in the counter-ions exist in the concentration polarization layer and/or cake layer, which provide an increasing effect of the concentration gradient. The absolute values of the streaming potential coefficient at an outlet of the hollow-fiber are

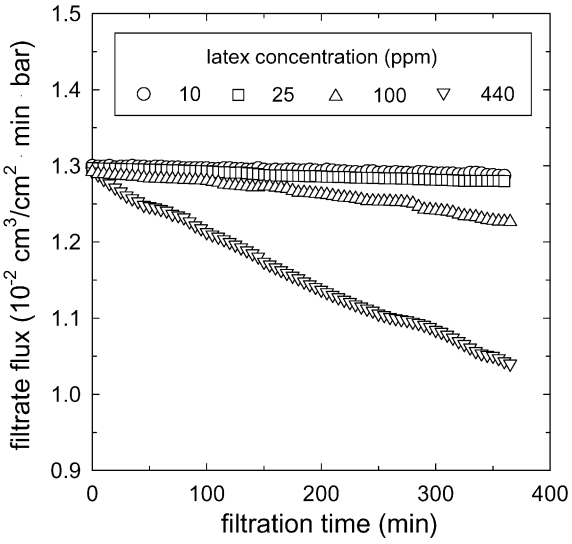

Fig. 5. Changes in the filtrate flux of hollow-fiber membrane during the cross-flow filtration with different latex concentrations (=C_b) at pH 8.6 and 1.0 mM KCl.

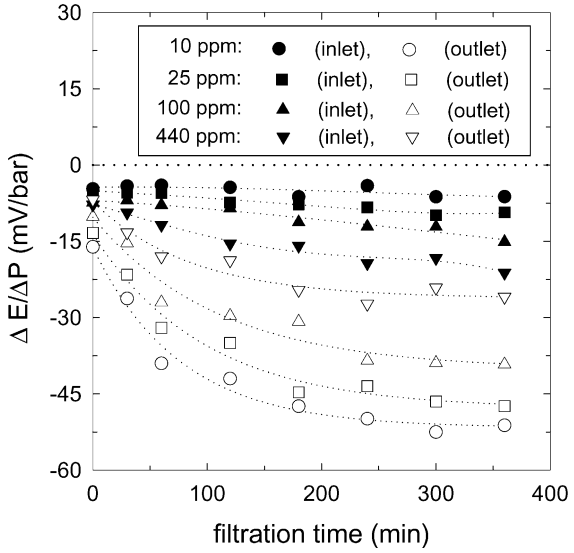

Fig. 6. Changes in the streaming potential coefficient of hollow-fiber membrane during the cross-flow filtration with different latex concentrations (=C_b) at pH 8.6 and 1.0 mM KCl.

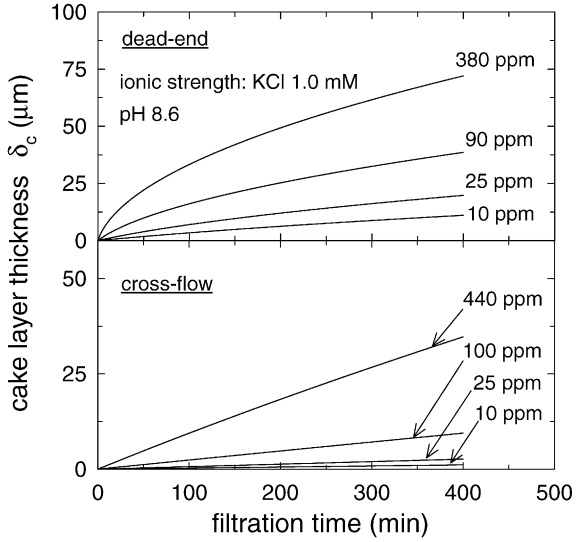

Fig. 7. The variation of cake layer thickness for both dead-end and cross-flow modes with filtration time at different latex concentrations.

higher than those found at an inlet, since the development of axial-dependent concentration polarization of latex particles increases as it goes to the outlet position.

As the latex concentration increases, the absolute value of the streaming potential coefficient at an inlet of the hollow-fiber increases, and its time evolution displays an increasing trend. This behavior results from the absence of cake layer at an inlet. At an outlet, the thickness of concentration polarization layer is larger than at an inlet, and further the cake layer may be formed for higher concentration of the latex particle. Therefore, it is observed that the value of streaming potential coefficient decreases at an outlet, and its increasing trend as the time progress is gradually disappeared as shown in Fig. 6. For longer filtration time, the decreasing behavior can be expected like the case of dead-end filtration.

4.3. Cake layer characteristic

Since a trend of flux decline provides information on the concentration polarization as well as the cake layer developments during the colloid filtrations, we consider the mechanism of filtration flux. From the mass balance of particles during the dead-end filtration, an ordinary differential equation for cake layer thickness $\delta_c(t)$ is generated [2,3]. Performing the integration in terms of $d\delta_c(t)/dt$ with the initial condition yields the filtrate flux and the cake thickness:

$$v(t) = \frac{\Delta P - \Delta P_p}{\eta R_m} \frac{1}{\sqrt{1 + \Xi t}} \tag{4}$$

$$\delta_c(t) = \frac{R_m}{\hat{R}_c}[\sqrt{1 + \Xi t} - 1] \tag{5}$$

where

$$\Xi = \frac{2\hat{R}_c C_b(\Delta P - \Delta P_p)}{(C_c - C_b)\eta R_m^2} \tag{6}$$

The membrane resistance R_m is determined from the water flux, depending on the mean pore radius and the surface porosity.

Fitting the variations of filtrate flux with Eq. (4) determines the factor Ξ, and then we favorably obtain the cake layer thickness $\delta_c(t)$ as well as the particle concentration in the cake. The variations of $\delta_c(t)$ with the filtration time at different particle concentrations are shown in Fig. 7, in which the dead-end mode has higher $\delta_c(t)$ compared to the cross-flow one. The trend of growing a cake layer can be understood

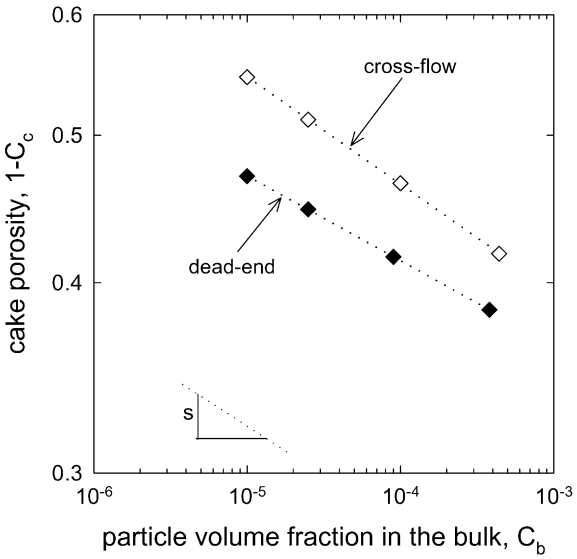

Fig. 8. The variation of cake porosity with latex concentration for both dead-end and cross-flow filtrations, where the log–log scale is used.

from Eq. (5), which means a $t^{1/2}$ dependence of the cake layer thickness. The cake layer thickness increases as the latex concentration C_b increases, owing to a fully retentive characteristic of PM10 membrane for latex particles.

The increased latex concentration leads to increasing of the cake layer thickness as well as of the packing density in the cake layer (i.e., C_c), and accordingly the filtrate flux decreases with higher flux decline. As expected, Fig. 8 shows that the cake porosity (i.e., void fraction of the cake layer) in cross-flow mode is higher than in dead-end one, identifying the development of loosely packed cake layer during the cross-flow filtration. The decreasing behavior of the cake porosity shows a power s dependency of latex concentration C_b (i.e., C_b^s), where the absolute value of s is estimated as 0.056 and 0.071 for dead-end and cross-flow filtrations, respectively.

5. Conclusions

The charge characteristics of the membranes were observed by applying the apparent streaming potential based on the H–S equation. The susceptible time evolution of the electrokinetic streaming potential allows us to explicitly understand the behavior of particle deposition onto fully retentive membrane surfaces associated with both the concentration polarization and the cake layers. Note that there is a competing aspect in the streaming potential evolution. A weak electrokinetic flow through the flat-plate membrane pores due to a stronger development of the cake layer results in the decreasing of magnitude of streaming potential with the progress of dead-end filtration of latex colloids. In contrast, the characteristic of the cross-flow has the charged latexes exist mainly in the concentration polarization layer instead of being deposited onto the outer surface of the charged hollow-fiber. As a consequence, the increasing effect of the concentration gradient prevails in cross-flow filtration.

The cake formation due to particle deposition can be evaluated from experimental results of filtrate flux, with which the trend of streaming potential is faithfully identified. We observed both the cake layer thickness and the particle concentration in the cake layer for dead-end case show higher values compared to those for cross-flow one. In any case, the decreasing behavior of the cake porosity shows the power dependence of latex concentration. We also found that the axial-position-dependent streaming potential for dilute particle concentration becomes generally increasing as it goes to the downward direction of the hollow-fiber.

Acknowledgements

This work was supported by the Basic Research Fund (Grant No. R01-2001-000-00411-0) from the Korea Science and Engineering Foundations (KOSEF) and the Eco-Technopia-21 Project (Grant No. 070010020) from the Korea Ministry of Environment.

Nomenclature

a	particle radius (m)
c_i^0	concentration of ion species i (mol/m^3)
C	particle volume fraction (–)
C_b	particle volume fraction in the bulk (–)
C_c	particle volume fraction in the cake layer (–)
e	elementary electrostatic charge (C)
E	streaming potential (V)
k	Boltzmann's constant (J/K)
N_A	Avogadro's number (mol^{-1})
N_{Fc}	critical filtration number (–)
ΔP	transmembrane pressure drop (N/m^2)
ΔP_p	pressure drop on the polarization layer (N/m^2)
R_c	cake resistance (m^{-1})
$\hat{R}_c$	specific cake resistance (m^{-2})
R_m	membrane resistance (m^{-1})
s	power index (–)
t	filtration time (s)
T	absolute temperature (K)
v	filtrate flux (m/s)
Z_i	valence of ion species i (–)

Greek letters

δ_c	cake layer thickness (m)
ε	dielectric constant (C/(V·m))
ζ	zeta potential (V)
η	viscosity of the solution (kg/(m·s))
κ	inverse Debye length (m^{-1})
λ_0	bulk solution conductivity (S/m)
Ξ	a factor defined in Eq. (6) (s^{-1})

References

[1] G.B. van den Berg, C.A. Smolders, The boundary-layer resistance model for unstirred ultrafiltration: a new approach, J. Membr. Sci. 40 (1989) 149–172.
[2] L. Song, Flux decline in crossflow microfiltration and ultrafiltration: mechanisms and modeling of membrane fouling, J. Membr. Sci. 139 (1998) 183–200.
[3] R.H. Davis, Modeling of fouling of cross-flow microfiltration membranes, Sep. Purif. Meth. 21 (1992) 75–126.
[4] P. Bacchin, D. Si-Hassen, V. Starov, M.J. Clifton, P. Aimar, A unifying model for concentration polarization, gel-layer formation and particle deposition in cross-flow membrane filtration of colloidal suspensions, Chem. Eng. Sci. 57 (2002) 77–91.
[5] W.R. Bowen, F. Jenner, Dynamic ultrafiltration model for charged colloidal dispersions: a Wigner–Seitz cell approach, Chem. Eng. Sci. 50 (1995) 1707–1736.
[6] W.R. Bowen, X. Cao, P.M. Williams, Use and elucidation of biochemical data in the prediction of the membrane separation of biocolloids, Proc. Royal. Soc. London Ser. A: Math. Phys. Eng. Sci. 455 (1999) 2933–2955.
[7] M.-S. Chun, W.R. Bowen, Rigorous calculations of linearized Poisson–Boltzmann interaction between dissimilar spherical colloids and osmotic pressure in concentrated dispersions, J. Colloid Interf. Sci. 272 (2004) 330–339.
[8] M.-S. Chun, G.-Y. Chung, J.-J. Kim, On the behavior of the electrostatic colloidal interaction in the membrane filtration of latex suspensions, J. Membr. Sci. 193 (2001) 97–109.

[9] C. Causserand, M. Nyström, P. Aimar, Study of streaming potentials of clean and fouled ultrafiltration membranes, J. Membr. Sci. 88 (1994) 211–222.
[10] K.J. Kim, A.G. Fane, M. Nyström, A. Pihlajamäki, W.R. Bowen, H. Mukhtar, Evaluation of electroosmosis and streaming potential for measurement of electric charges of polymeric membranes, J. Membr. Sci. 116 (1996) 149–159.
[11] L. Ricq, A. Pierre, J.-C. Reggiani, J. Pagetti, A. Foissy, Use of electrophoretic mobility and streaming potential measurements to characterize electrokinetic properties of ultrafiltration and microfiltration membranes, Colloids Surf. A: Physicochem. Eng. Aspects 138 (1998) 301–308.
[12] A. Szymczyk, B. Aoubiza, P. Fievet, J. Pagetti, Electrokinetic phenomena in homogeneous cylindrical pores, J. Colloid Interf. Sci. 216 (1999) 285–296.
[13] L. Ricq, S. Narcon, J.-C. Reggiani, J. Pagetti, Streaming potential and protein transmission ultrafiltration of single proteins and proteins in mixture: β-lactoglobulin and lysozyme, J. Membr. Sci. 156 (1999) 81–96.
[14] I.H. Huisman, E. Vellenga, G. Trägårdh, C. Trägårdh, The influence of the membrane zeta potential on the critical flux for crossflow microfiltration of particle suspensions, J. Membr. Sci. 156 (1999) 153–158.
[15] M.C. Wilbert, S. Delagah, J. Pellegrino, Variance of streaming potential measurements, J. Membr. Sci. 161 (1999) 247–261.
[16] I.H. Huisman, P. Prádanos, A. Hernández, Electroviscous effects, streaming potential, and zeta potential in polycarbonate track-etched membranes, J. Membr. Sci. 179 (2000) 79–92.
[17] P. Fievet, A. Szymczyk, C. Labbez, B. Aoubiza, C. Simon, A. Foissy, J. Pagetti, Determining the zeta potential of porous membranes using electrolyte conductivity inside pores, J. Colloid Interf. Sci. 235 (2001) 383–390.
[18] J.H. Sung, M.-S. Chun, H.J. Choi, On the behavior of electrokinetic streaming potential during protein filtration with fully and partially retentive nanopores, J. Colloid Interf. Sci. 264 (2003) 195–202.
[19] W.B. Russel, D.A. Saville, W.R. Schowalter, Colloidal Dispersions, Cambridge University Press, New York, 1989.
[20] C.J. van Oss, Interfacial Forces in Aqueous Media, Marcel Dekker, New York, 1994.
[21] C.L. Rice, R. Whitehead, Electrokinetic flow in a narrow cylindrical capillary, J. Phys. Chem. 69 (1965) 4017–4024.
[22] R.J. Hunter, Foundations of Colloid Science, 2nd ed., Oxford University Press, London, 2001.
[23] A.E. Yaroshchuk, Y.P. Boiko, A.L. Makovetskiy, Filtration potential across membranes containing selective layers, Langmuir 18 (2002) 5154–5162.
[24] M. Elimelech, S. Bhattacharjee, A novel approach for modeling concentration polarization in crossflow membrane filtration based on the equivalence of osmotic pressure model and filtration theory, J. Membr. Sci. 145 (1998) 223–241.
[25] M.-S. Chun, J.-J. Kim, S.-Y. Lee, Equipment and method of local streaming potential measurement for monitoring the process of membrane fouling in hollow-fiber membrane filtrations, US Patent 6,727,099 B2 (2004).
[26] M. Fontyn, K. van't Riet, R.H. Bijsterbosch, Surface spectroscopic studies of pristine and fouled membranes. Part 1. Method development and pristine membrane characterization, Colloids Surf. 54 (1991) 331–347.